Modelling the viral load dependence of residence times of virus laden droplets from COVID-19 infected subjects in indoor environments

Srinivasan Anand (sanand@barc.gov.in)
Bhabha Atomic Research Centre
Jayant Krishan
Bhabha Atomic Research Centre
Sreekanth Bathula
Bhabha Atomic Research Centre
Yelia S Mayya
Indian Institute of Technology Bombay

Article

Keywords: COVID-19, aerosol, residence time, evaporation, indoor transport

Posted Date: January 11th, 2021

DOI: https://doi.org/10.21203/rs.3.rs-143753/v1

Version of Record: A version of this preprint was published on June 12th, 2021. See the published version at https://doi.org/10.1111/ina.12868.

Modelling the viral load dependence of residence times of virus laden droplets from COVID-19 infected subjects in indoor environments

Srinivasan Anand[1,3], Jayant Krishan[1], Bathula Sreekanth[2,3], Yelia S Mayya[4,*]

[1]Health Physics Division, [2]Radiation Safety and Systems Division, Bhabha Atomic Research Centre, Mumbai – 400085, India.

[3]Homi Bhabha National Institute, Bhabha Atomic Research Centre, Mumbai – 400094, India.

[4]Department of Chemical Engineering, Indian Institute of Technology Bombay, Mumbai – 400076, India.

*Corresponding author:

Email: ysmayya@iitb.ac.in; ysmayya@gmail.com

Abstract

In the ongoing COVID-19 pandemic situation, exposure assessment and control strategies for aerosol transmission path are feebly understood. A recent study pointed out that Poissonian fluctuations in viral loading of airborne droplets significantly modifies the size spectrum of the virus laden droplets (termed as "virusol"). Herein we develop theory of residence time of the virusols, as contrasted with clean droplets in indoor air using a comprehensive "Falling-to-Mixing-plateout" model that considers all the important processes. This model fills the existing gap between Wells falling drop model and the stirred chamber models. The effect of various parameters on mean residence time are examined in detail. Significantly, the mean residence time of virusols is found to increase nonlinearly with the viral load in the ejecta, ranging from ~125 s at low viral loads ($<10^4$/mL) to about 1150 s at high viral loads ($>10^{11}$/mL). The implications are further discussed.

Keywords

COVID-19, aerosol, residence time, evaporation, indoor transport

Highlights

- Comprehensive “Falling-to-Mixing-plateout” model from emission to exposure
- Strong dependence of mean residence time of virus laden aerosols on the viral load
- Residence time is lower for virusol system when compared to complete droplet system
- Virusol system settle down faster than the complete droplet system
- Residence time for disease control in indoor environment and risk assessment

Graphical Abstract

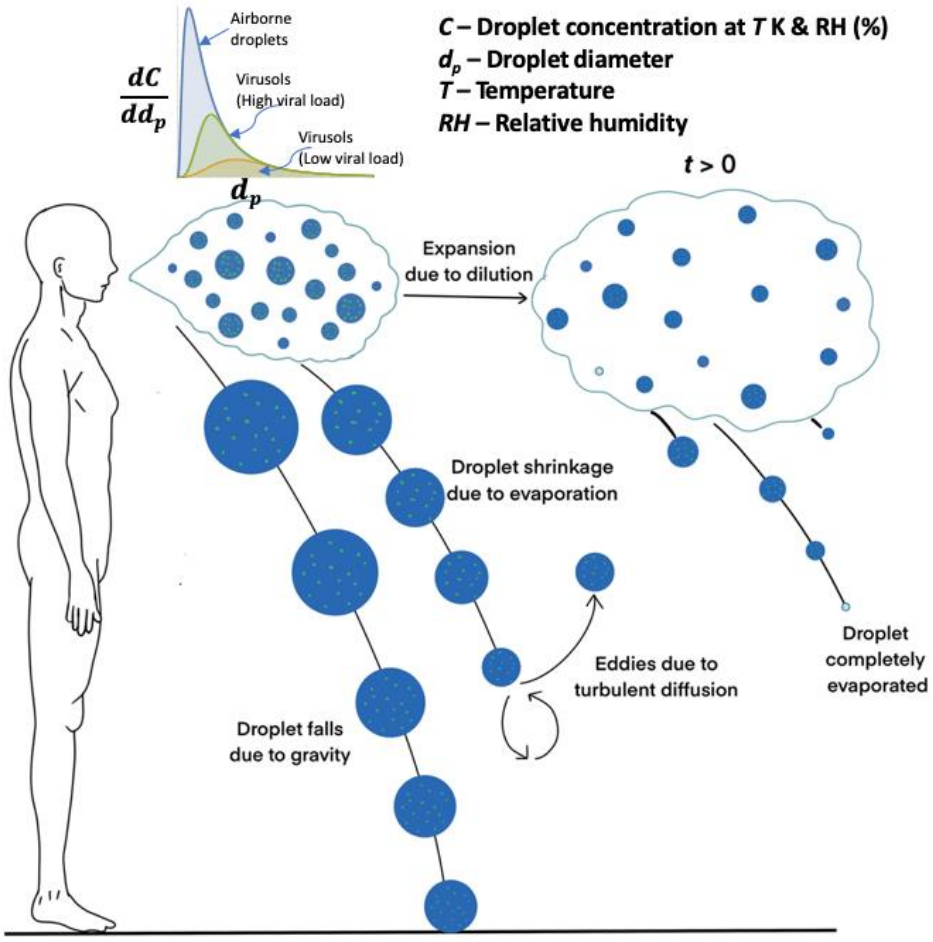

Introduction

The outbreak of COVID-19 disease at superspreading events intensifies the scientific discussion on the airborne infection transfer mechanism responsible for the global spread of this disease (1–4); most of all for combating strategies and then to the issue of rebooting economic activity. Limited information is available on the formation of virus laden droplets/aerosols, dispersion and evaporation of expiratory droplet cloud in the indoor environment (5, 6). Furthermore, there is a wide variation in the input parameters such as droplet size distribution, concentration, volume of expiratory fluid, release conditions, etc. Accordingly, considerable amount of uncertainty is associated with modelling practices used for inhalation exposure assessment. Although there are few methods of exposure assessment are available in the literature (7–9), it is necessary to address larger scientific questions which form the basis of these calculations. In this letter, we wish to focus on the issue of residence time of cough droplet and droplet nuclei, ejected from the expiratory activity of infected subjects as localized puff to start with, in an indoor space. The residence times are not only important for exposure assessment, but are also important for assessing the performance of air cleaners, or for deciding the minimum level of Clean Air Delivery Rate (CADR) expected of them, as effective intervention technologies for minimizing the infection transfer risks in confined environments.

Generally, the mean residence time is derived from the reciprocal of the removal rate, which is a concept based on uniformly mixed chamber models (10). This concept is best suited for fine aerosol particles of about 1 μm or less, predominantly occurring in the context of indoor pollution. On the other extreme is the models of residence time for falling-evaporating droplets, as described by Wells (11) long ago and revisited with considerable mathematical precision by Xie et al. (12), which are best suited to describe the fate of droplets of 20 μm or more. There is a wide gap in modelling the residence time for droplets in the intervening size range (say, 5-

20 μm), which due to natural convective mixing in a room, will be undergoing dispersal in the air currents during their fall under gravity, and cannot be described by either of the above models. With increasing concern expressed over the yet to be understood role of aerosol route of infection spread in the COVID-19 scenario, the assessment of the impact of size range is of considerable urgency. The first motivating factor for this paper is to formulate a model that smoothly transits from the falling droplet to a uniformly mixed chamber model (Falling-to-Mixing-Plate-out) across the entire size range of polydisperse droplets released in a cough.

A second and more important motivation for this study stems from the following consideration. In a recent paper (13), we pointed out that the size distribution metrics of corona virus-laden polydisperse droplets expirated from infected subjects, could be very different from the original droplet distributions, due to the well-known Poissonian fluctuations (13–17) in virus incorporation propensities into droplets at the time of their formation. To focus on this viral load dependent distinctiveness, a terminology "virusol" was proposed for the ensemble of virus laden droplets. From both exposure evaluation and control technology point of view, the residence times of the virusolized fraction is a matter of concern, and not that of the entire droplet population. The Poissonian theory shifts focus on larger size fraction effectively rendering the residence times sensitive to the viral load in the ejecta of subjects. Examining this dependence is an important aspect of this study.

Size distribution of expiratory droplets is one of the basic input parameter required to determine the lifetime of the virus laden droplets in the ambient environment. There are several experimental studies on the size distribution and concentration of expiratory droplets (7, 18–20). These studies show a large variation in the size distribution parameters of the droplets ejected from the infected subjects. Equally important is the data on viral load among patients and the variability across several findings have been summarized by Anand and Mayya (13).

The combined effect of size dispersity and viral load has complex influence on the life time of the virus laden droplets as we will see in this paper.

Computational Fluid Dynamics (CFD) is an increasingly adopted approach to address the transport of droplets along with their evaporative dynamic, from the point of emission to their settling on surfaces (21–24). In a strictly theoretical sense, this would be most accurate for modelling residence time distributions. However, CFD approaches are highly input parameter intensive. For example, to handle turbulence in a room it would be necessary to specify all the processes responsible for creating turbulence. It should then include both mechanical and thermal sources, and this would make the CFD models quite useful in specific contexts, but lack generic predictive power. To have generality, CFD would require averaging over large number of scenarios before arriving at the reasonable estimates of a representative droplet residence time. On the other hand, phenomenological model based on turbulent diffusion as the governing transport mechanism in addition to gravitational settling, addresses the dispersive mechanisms directly through an assumed diffusion coefficient and hence will be more robust in providing generic estimates of the residence times distributions. Besides, treating droplet transport within the framework of an assumed bulk diffusion process obviates the need to examine the origin of its occurrence for the purposes of describing the migration dynamics of the droplets. Equally importantly, turbulent bulk diffusion models are amenable to analytical solutions for falling droplets which is useful for comparison purposes for providing insights into the role of individual processes.

In the phenomenological approach, the emitted droplet begins to disperse in bulk space as it settles under gravity simultaneously evaporating and undergoing wall removal processes. The removal rates are matched with the boundary conditions using Lai and Nazaroff model (10). This phenomenological model integrates smoothly the wall removal as well as air exchange removal without having to concern about the points of air entry and exit for various

realistic emission scenarios. We term it as residence time distribution problem since the released droplets are not uniformly mixed in the indoor environment, and the inverse of the mean residence time is equivalent to the removal rate of uniformly mixed model. The dynamics of these evaporating and settling virusol puff is studied under different conditions by varying the important input parameters such as relative humidity, differential temperature between the droplet and ambient atmosphere, release height, bulk turbulent coefficient, friction velocity, initial droplet size distribution, multi-component nature of the droplets, and viral load in the biological fluid. The issue of the dependence of the mean residence time of virus laden droplets (virusols) on the viral load forms a key component of our analysis.

Materials and Methods

Let us consider an expiratory event in which droplets of initial concentration (N_0) is released from an infected person at a height (z_0) in a closed environment (Fig.1). The convective diffusive expansion of the puff containing airborne droplets is modelled using the mixing transition model, which combines homogeneous mixed room model with falling droplet model seamlessly. Many researchers (6, 25, 26) argue that the cut-off diameter for the aerosol definition in the present context should be a single discrete number (ex. <5 μm or <20 μm). However, in the present study, a higher cut-off diameter (100 μm) is considered so that the transition to inhalable aerosol size from evaporation of continuous size spectrum of ejected droplets can be modelled seamlessly.

Preliminary comparative analysis of the proposed 3-dimensional model with 1-dimensional version reveals that the differences in their results are very small for particles > 0.1 μm. The detailed derivation of analytical solution and comparison of 1-D and 3-D models are presented in Supplementary Information. Significant differences are observed in the case of ~10 nm particles, which is of least interest in the present study. Hence, for all large droplet simulations with air mixing condition, 1-D model (along the direction of gravity) will be good

enough and it yields results very close to 3-D model. In the case of one-dimensional model, the rate of change of droplet concentration (C) in the vertical direction (z) due to turbulence, gravitational settling and inactivation of viruses in the droplets is given by,

$$\frac{\partial C(z,t)}{\partial t} = D\frac{\partial^2 C(z,t)}{\partial z^2} + V_g\frac{\partial C(z,t)}{\partial z} - \lambda\, C(z,t) \quad (1)$$

where, D is the bulk diffusion coefficient along z-direction due to turbulence, V_g is the gravitational settling velocity, and λ is the virus decay rate (0.63 h^{-1} (27)). In the given coordinate system, ground and roof levels of the indoor environment are represented by $z = 0$ and $z = H$ respectively. The initial and boundary conditions are,

IC: $C(z,0) = N_0\delta(z - z_0)$ (2a)

BC1: $D\frac{\partial C(0,t)}{\partial z} + V_g\, C(0,t) = (V_D^+ + 0.5\,\lambda_v\, H)\, C(0,t)$ (2b)

BC2: $D\frac{\partial C(H,t)}{\partial z} + V_g\, C(H,t) = -(V_D^- + 0.5\,\lambda_v\, H)\, C(H,t)$ (2c)

where, $V_D^+, and\ V_D^-$ are the deposition velocities on floor and roof respectively, obtained from boundary layer models (10). These deposition velocities depend on the bulk diffusion coefficient, D. λ_v is the ventilation or air-exchange rate (AER) of the indoor environment, an empirical expression relating AER and bulk diffusion coefficient (23) is given by, $D\ (m^2/s) = (0.52\,\lambda_v + 8.61\times10^{-5})\, V^{\frac{2}{3}}$, where, V is the room volume (m^3). Eqs.(2b) and (2c) accounts for the loss of droplets/particles due to surface deposition on the floor $(z = 0)$ and roof $(z = H)$ of the indoor environment respectively, gravitational settling, and ventilation removal. The ventilation removal from the enclosure is handled through similar boundary conditions (Eqs. 2b & 2c) at each of the surfaces. In 3-dimensional model, factor of $1/6^{th}$ is used to account for surface deposition through all the six surfaces.

The integration of solution of Eqs.(1-2) over the spatial domain gives the droplet/aerosol volume concentration survive in air at any time t. If N_0 is the total number of

particles released at time $t = 0$, then the mean residence time of the expiratory droplets in air is prescribed as,

$$\bar{T} = \frac{1}{N_0} \int_{t=0}^{\infty} \int_{z=0}^{H} C(z,t) dz\, dt \tag{3}$$

The definition of residence time is more general compared to the lifetime definition used in single exponential decay expressions. In the latter case, The mean residence time refers to time required to decrease $1/e^{\text{th}}$ of original concentration, equivalent to ~63% removal in the single exponential decay process. Eq.(3) is a measure of multi-exponential decay due to various processes acting on the removal/survival of the expiratory droplets.

The equations of evaporation, vertical motion and temperature of individual droplets are solved independently, and they are coupled together with the solution of mixing transition model through gravitational settling velocity (V_g). The governing equations that describe the vertical motion of the evaporating and settling droplets are given by,

$$\frac{dN_w}{dt} = -4\pi\, R(t)\, Sh(t)\, D_{H_2O} \left\{ \frac{N_w(t)}{N_T(t)} \frac{p_d(t)}{k_B\, T_d(t)} - \frac{p_{amb}}{k_B\, T_{amb}} \right\} \tag{4}$$

$$\frac{d\, T_d}{dt} = \frac{3\, k_g\, [T_{amb} - T_d(t)]\, Nu(t)}{c_{H_2O}\, \rho_{eff}(t)\, R^2(t)} + \frac{L_{H_2O}\, M_{H_2O}}{c_{H_2O}\, m(t)} \frac{dN_w}{dt} \tag{5}$$

$$\frac{dV_g}{dt} = g - \frac{V_g(t)\, [Stk(t)\, Drag(t) - \dot{m}(t)]}{m(t)} \tag{6}$$

where, N_w is the number of water molecules in the airborne droplets, $R(t)$ is the droplet radius, $Sh(t)$ is the Sherwood number (ratio of convective mass transfer to the mass diffusivity), given by, $Sh(t) = 1 + 0.3 \sqrt{Re(t)} \left(\frac{\nu_k}{D_{H_2O}} \right)^{1/3}$, $Re(t) = 2\, V_g(t)\, R(t)\, \nu_k$ is the Reynolds number, $N_T(t)$ is the total number of molecules (non-volatiles/residue + water) in the droplet, and $p_d(t)$ is the equilibrium vapor pressure of water in the droplet at temperature $T_d(t)$. $Nu(t)$ is the Nusselt number used to correct the convective heat transfer rate, given by, $Nu(t) = 1 + 0.3 \sqrt{Re(t)} \left(\frac{c_{air}\, \eta}{k_g} \right)^{1/3}$, $Stk(t) = 6\pi\, \eta\, R(t)$ is the Stokes friction coefficient, $Drag(t) = 1 +$

$0.15\ (Re(t))^{0.687}$ is the drag correction factor, and $\dot{m}(t)$ is the rate of change of droplet mass with respect to time due to evaporation. The water vapour pressure at a given temperature (Antoine equation) is given by,

$$\log_{10} p_{d/amb}(t) = A - \frac{B}{T_{d/amb}(t)+C} \tag{7}$$

where, A, B and C are constants and T is the temperature in ^{0}C, suffices d and amb refers to droplet and ambient respectively.

The droplets undergo evaporation in a homogeneous temperature T_{amb} with a constant ambient water vapor pressure p_{amb} at a given relative humidity, till they reach equilibrium conditions. The evaporation model neglects the effect of Stefan flow on heat and mass transfer between the droplet and the surrounding gas since this effect leads to less than 0.5% change in the model variables. The airborne droplets in the puff are assumed to be spherical particles consist of non-volatile components such as Na+, K+, Cl- ions, and lactate and glycoproteins (about 0.71% mole fraction) with water as a major constituent.

The total volume (number) and size distribution of droplets per unit volume of exhaled gas largely depend on the expiratory activities and it is an important input parameter to this model. The droplet size distribution functions are generally obtained by fitting the measurement data using two-parameter lognormal distribution characterised by median diameter and its corresponding geometric standard deviation. In the present study, the lognormal distribution of droplet number concentration is given by,

$$\frac{dC}{dd_p} = \frac{N_0}{\sqrt{2\pi}\, d_p \log\sigma_g} exp\left\{-\frac{1}{2}\left(\frac{\log d_p - \log CMD}{\log\sigma_g}\right)^2\right\} \tag{8}$$

where, N_0 is the total number of droplets ejected, CMD is count median diameter, and GSD is geometric standard deviation.

Since atomization is the method of droplet ejection from the infected subject, the probability of viral load in each droplet will depend on the virus concentration (v_c) in the

biological fluid and droplet size (14, 28). To distinguish the virus laden droplets from the complete airborne droplet size distribution, the term 'virusol' is coined for the aerosol studies related to virus infected diseases (13). Many studies show that the presence of viral copies in the smaller size droplets are negligible for virus concentration v_c<10^6 RNA copies/mL using the Poisson probability theory (13, 14, 16, 17), and thus, the probability of a droplet of diameter d_p carrying at least one virus (RNA) copy is given by,

$$P = 1 - exp\left(-\frac{\pi}{6} d_p^3 \, v_c\right) \quad (9)$$

The virusol droplet number distribution is then obtained by multiplying the number size distribution $\left(\frac{dC}{dd_p}\right)$ with P at any instant of time t. It is observed that the variation of virus concentration in the biological fluid is very wide (10^2 – 10^{11} RNA copies/mL), and studies indicate that there is a possible linkage of viral load with severity of disease (29). Based on data, we approximately classify viral load into two categories, i.e., (i) mild-to-moderate cases - <10^6 RNA copies/mL and (ii) severe cases - >10^6 RNA copies/mL.

Results and Discussion

The dispersion of a puff containing virus laden droplets and aerosols exhaled during a cough expiratory event by an infected subject is analysed using one-dimensional model described in the Materials and Methods Section. The puff is released at a height of 1.5 m (represents the elevation of infected subject's standing position) in an indoor environment of volume 48 m^3 (Height of the room – 3 m) having an air-exchange rate of 1.0 h^{-1}, representing a typical office environment. We consider the puff of cough droplets with a temperature of 35^0C, is released in to an environment at ambient temperature of 25^0C at 50% RH, ideal condition for comfort working environment. A total number of 5000 droplets with lognormal number-size distribution (CMD = 14 μm and GSD – 2.6) is considered in this study. These expiratory droplets contain residues (7), settle by gravity while evaporating in ambient air.

Other important input parameters/constant and their range are given in Table S2. All the governing equations are numerically solved together in the Mathematica (30).

Early works of Wells (11) and other studies (12, 31, 32) highlights the dependence of lifetime of the droplets on ambient parameters such as temperature, relative humidity, air speed, and droplet properties such as its size, constituents and temperature. The falling droplet evaporation model considers the droplet evolution processes in a localised space without considering the boundary wall deposition and ventilation effects. Also, some of these models does not consider detailed droplet composition, and hence, large variation in the final droplet diameters (~20-50% of the initial values) which will lead to considerable error in the modelling of airborne droplet concentration. On the other hand, homogeneously mixed model (10) assumes uniform mixing of expiratory droplets/aerosols in the indoor volume immediately. This model lacks handling of spatial variation of the aerosol concentration that affects other accompanied processes. A study is carried out to compare these two models with the present formulation for non-evaporating rigid droplets released at a height of 0.3 m in an indoor room environment with a ventilation rate of 0.5 h^{-1}. The results are presented in the Fig.2. From Fig.2, it is quickly apparent that neither falling droplet model nor homogeneously mixed chamber model could adequately describe all the effects if we include coarse as well as submicron particles for assessing risks. The present model (Eqs.(1-9)) results shows smooth transition of residence time from the falling evaporating model to uniform mixing model as illustrated in Fig.2. These results confirm that the present approach seamlessly integrates all the important processes that governs the residence time of virus laden droplets and aerosols in a typical indoor environment.

The rate of evaporation of droplets and its composition determines the final size of airborne droplets/aerosols (virusols) which play key role in governing their residence time in indoor atmosphere. To study these effects, the virusols residence time are estimated at different

RH, and compared with that of droplets without solute. The temporal evolution of single droplet diameter (14 μm is chosen since its CMD of the cough droplets considered in this study) at different RH and composition is shown in Fig.3a. At a lower RH (10%), the water vapor content in the atmosphere and hence the rate of evaporation is highest. So, the droplet quickly evaporates and reaches a steady size value (~6 μm) in a time period of 0.12 s and 0.3 s for a RH value of 10% and 50% respectively. At higher RH values (90%), the evaporation rate is least due to the saturated vapour pressure in the indoor environment and hence, it takes more time (> 1 s) to reach the final size. Thus, the results (timescale) clearly show that it is important to integrate the evaporation process with other processes described in the governing equations.

Apart from the atmospheric conditions, the composition of the droplet also plays an important role in determining the rate of evaporation and final size of the droplet. The presence of salt (residue) content reduces the vapour pressure of water thereby leading to lower rate of evaporation and larger final size of the droplet. The comparison of variation of droplet size as a function of time for RH = 50% clearly indicates this fact as the final size reaches to 6.1 μm in the presence of solute while the pure water droplet evaporates completely in ~0.3 s (Fig.3a). The rate of evaporation of droplet thus depends on the volatile content of the droplet along with the ambient conditions.

Furthermore, final size of all the droplets as a function of initial droplet size is presented in Fig.3b. The overall reduction in the final size is about ~55 % for all particle sizes (i.e. droplet with a size of 100 μm reduces to ~45 μm) in the case of RH < 50 % and for the given residue composition. This size reduction is more pronounced if solute content in the saliva is reduced as discussed above. It is to be noted that the initial droplet may be large enough to settle down under the force of gravity but simultaneous evaporation will reduce the size significantly (depending upon the atmospheric conditions), thereby reducing the gravitational effects and leading to higher residence time in air.

The effect of AER on virusol mean residence time is studied with two different relationship of AER vs D ((i) D as a function of AER given by (23), and (ii) D is independent of AER), is shown in Fig.4. The bulk diffusion coefficient varies from ~10^{-3} m^2/s to 1.1 x 10^{-2} m^2/s for AER of 0 to 5 h^{-1} in a room volume of 48 m^3. The virusol mean residence time decreases from 960 s to 410 s as the AER increases from 0 h^{-1} to 5 h^{-1}, in the case of $D \propto$ AER. For the constant D case, the variation of mean residence time is from 1040 s (0 h^{-1}) to 500 s (5 h^{-1}). These results show that the virusol mean residence time decreases monotonically when the AER increases, however the reduction is only 0.43 times when the AER is increased from 0 h^{-1} to 5 h^{-1}. Hence, large AER is required to reduce the virusol exposure significantly.

The virusol mean residence time of droplets as a function of initial droplet size is compared for different heights of release which may arise due to position of the person (sitting (z_0 – 0.3 m) or standing (z_0 – 1.5 m)) during an expiratory event. The MRT of the virusols varies from few seconds to hours for droplets of different sizes from 0.4 to 100 µm (Fig. 5). Higher size droplets settle faster due to gravitational effects and smaller size droplets have largest residence time in air as expected. As the release height increases, the corresponding residence time of the droplets also increases for sizes >10 µm as the settling distance increases with height (~7 times increase in the residence time for 100 µm droplet between 0.3 m and 1.5 m release heights). In the case of smaller size particles (~2500 s for aerosols <10 µm for AER of 1.0 h^{-1}), MRT difference is not significant w.r.to z_0 as the removal of these particles are predominantly due to diffusion and ventilation, and hence, residence times of smaller size virusols are independent of height of release. On the other hand, the study results show that the ventilation rate strongly affects residence time of smaller size virusols compared to larger ones (Fig.5). At smaller sizes, the lower ventilation rate leads to highest virusol residence time (~6000 s for an AER of 0.001 h^{-1}) compared to high ventilation rate (~700 s for an AER of 5 h^{-1}) for particles < 5 µm. Since AER is linearly related to bulk diffusion coefficient (23),

combined effect of ventilation removal and convective diffusion determines the survival of airborne particles in the indoor atmosphere. Also, the effect of AER is negligible in the large particle size domain due to other competing processes such as evaporation and gravitational settling acting on them. The effect of friction velocity on residence time of the virusols is insignificant as the study shows that the variation of virusol residence time is within 4% if the friction velocity varies from 1 cm/s to 5 cm/s.

Viral concentration in the biological fluid and the process of incorporation of virus in the expiratory droplets/aerosols plays a crucial role in determining the total residence time of virus laden airborne particles, which is addressed through the concept of virusols. Most of the studies consider virus load in the airborne droplet as linearly proportional to the droplet volume. However, the atomized droplets during the expiratory activity shows that the presence of virus in the expiratory droplets/aerosols is a function of viral concentration and droplet size, and it is governed by the Poisson distribution as given by Eq. (9).

The initial and final (at t = 100 s) number-size distribution of virusols are compared with initial complete droplet size spectrum in Fig.6. The complete droplet spectrum which has CMD of 14 μm contains the droplets/aerosols starting from ~0.3 μm onwards with viral load proportional to their volume without considering the Poisson distribution of virions in the droplets. On the other hand, it is very clear from Fig.6 that the introduction of Poisson probability limits the lower particle size of virusols, and the probability of the droplet being virus laden (virusol) increases with its size. For example, the initial virusol number-size distribution (at t = 0) shows that the lower cut-off virusol diameter is ~5 μm and ~1 μm for viral load of 10^8 and 10^{11} RNA copies/mL (corresponding to severe cases) respectively. This shows that there is very low probability that smaller droplets will contain any virus in the case of low viral load (mild-to-moderate cases) in biological fluid (ex. saliva). It is interesting to note that although there is a large difference in the lower side of the size spectrum between

complete droplets and virusols, higher side of the size spectrum is same in all the cases. This is due to the fact that the value of P (Eq. (9)) tends to 0 for large droplets of size > 40 μm. Comparison of number-size distribution at t = 100 s with other initial size spectra shows that most of the particles greater than ~70 μm are removed from the system mainly due to gravitational settling; also, evaporation process plays an important role in shifting the droplet spectrum in the range of (22-70) μm significantly (Fig.6).

We further study the effect of virus concentration on the residence time and exposure for a wide range of fluid concentration from 10^3 – 10^{13} RNA copies/mL, and the results are presented in Fig.7 for various RH. The virusol residence time varies from ~ 100 s (RH – 90% for viral load <10^6 RNA copies/mL) to ~1200 s (RH – 10% and viral load >10^{11} RNA copies/mL). The results further show that MRT of virusols in the severe cases (viral load > 10^{11} RNA copies/mL) is eight times to that of mild-to-moderate cases (< 10^6 RNA copies/mL) for RH = 50%, and this ratio increases with RH. As RH increases from 10% to 90%, the evaporation rate reduces which leads to larger final size of droplet; hence faster settling and smaller residence time. The study results show that the MRT of virusols increase with viral load and saturates to a constant value beyond 10^{11} RNA copies/mL for the given conditions, which clearly show larger dependence of virusol residence time on virus load.

The exposure to these virusols can be obtained from the mean residence time using the relationship, $\left(\frac{\bar{T}\ BR\ C_v}{V}\right)$, which is defined as the number of virions breathed in during MRT of virusols ($\bar{T}$), where, BR is the breathing rate (~10 lpm), V is the room volume, and C_v is the total virions released during the expiratory event. For example, if we consider a viral load of 10^6 RNA copies/mL (RH – 50%), then the mean residence time is 150 s (Fig.7) and corresponding exposure is 0.23 virions considering room volume of 48 m^3. This result shows that exposure to a single virion is possible only if the viral load in the biological fluid is more than 10^6 RNA copies/mL. However, if the viral load is 10^{10} RNA copies/mL (severe case), then

the mean residence time is 1050 s (Fig.7) and the corresponding exposure is 1.6 x 10^4 virions. These study results show that higher residence time and survival fraction would lead to higher exposure of person contracting the virus, beyond a certain cut-off viral load in the biological fluid. The residence time of the droplets thus play a significant role in estimating the viral exposure to an individual, and it depends on many parameters such as particle size, viral load, process of incorporation of viral copies in the droplet, height of release, turbulent diffusion coefficient, AER, and RH.

Conclusions

The present conjoined model, "Falling-to-Mixing-plateout", smoothly transits from evaporating and falling droplet model (11) to mixed reservoir/all surface-plate out model (10) by considering all the important processes that govern the virusol residence time and exposure in an indoor environment. The residence time estimates from the conjoined model lie between that obtained by pure gravitational settling and classical surface-plate out model. The present 1-D model is good enough to quickly estimate virusol residence time and exposure to the individual as their results are closer to 3-D system, particularly for droplets > 0.1 μm. The present work thus provides a comprehensive theoretical study from the droplet emission to inhalation exposure using residence time estimates.

Study results indicate that virusol system residence times could be far less than that for the complete droplet cloud system, and smaller droplets (<20 μm) are more likely to be blanks in mild-to-moderate cases. Virusol system will settle down faster than the complete droplet system and hence less likely to be airborne when the biological viral load is <10^8 RNA copies/mL. This has important implications from an air cleaning perspective aimed at COVID-19 risk mitigation in enclosed spaces. It may not be necessary to capture ultrafine particles as these would be generally harmless; one may relax filtration efficiency criteria limiting them to essentially larger particles, thereby opting for coarser filters and reducing pressure drops and

increasing air circulation rates. This has far reaching implications in adopting intervention technologies in indoor spaces.

Also, there is a significant shift in geometric mean diameter of virusols as compared to that of the complete size spectrum and it has practical implication to risk assessment. On the whole, we have effectively demonstrated that virusol size distribution and residence times are distinctly different from the ensemble of total droplets and will be a critically useful concept both for intervention technologies and lung deposition modelling. These implications are under investigation.

Acknowledgements

Authors (SA & JK) would like to acknowledge Shri Kapil Deo Singh and Dr M S Kulkarni of Bhabha Atomic Research Centre for their support and encouragement. Authors would like to acknowledge Ms Riya Dey for preparation of the artwork (Figure 1).

Author Contributions

Y.S.M. and S.A. initiated the study and suggested the research method; S.A., and B.S. collected and analyzed data for the research method; J.K., Y.S.M., and S.A. performed numerical calculations and prepared figures; S.A., and Y.S.M. wrote the manuscript; B.S., and J.K. helped in preparation of the manuscript; All the authors reviewed the manuscript.

Competing Interest Statement

The authors declare no competing interests.

References

1. Y. Li, *et al.*, Evidence for probable aerosol transmission of SARS-CoV-2 in a poorly ventilated restaurant. *medRxiv*, (2020) 10.1101/2020.04.16.20067728.
2. D. Bonn, *et al.*, Probability of aerosol transmission of SARS-CoV-2. *medRxiv*, (2020) 10.1101/2020.07.16.20155572.
3. A. Peters, P. Parneix, J. Otter, D. Pittet, Putting some context to the aerosolization debate around SARS-CoV-2. *J. Hosp. Infect.* (2020) 10.1016/j.jhin.2020.04.040.
4. S. J. Dancer, *et al.*, Putting a balance on the aerosolization debate around SARS-CoV-2. *J. Hosp. Infect.* (2020) 10.1016/j.jhin.2020.05.014.
5. L. Morawska, Droplet fate in indoor environments, or can we prevent the spread of infection? *Indoor Air*, (2006) 10.1111/j.1600-0668.2006.00432.x.
6. E. L. Anderson, P. Turnham, J. R. Griffin, C. C. Clarke, Consideration of the Aerosol Transmission for COVID-19 and Public Health. *Risk Anal.* (2020) 10.1111/risa.13500.
7. M. Nicas, W. W. Nazaroff, A. Hubbard, Toward understanding the risk of secondary airborne infection: Emission of respirable pathogens. *J. Occup. Environ. Hyg.* (2005) 10.1080/15459620590918466.
8. M. P. Atkinson, L. M. Wein, Quantifying the routes of transmission for pandemic influenza. *Bull. Math. Biol.* (2008) 10.1007/s11538-007-9281-2.
9. G. Buonanno, L. Morawska, L. Stabile, Quantitative assessment of the risk of airborne transmission of SARS-CoV-2 infection: prospective and retrospective applications. *Environment International* 145, 106112 (2020) 10.1016/j.envint.2020.106112.
10. A. C. K. Lai, W. W. Nazaroff, Modeling indoor particle deposition from turbulent flow onto smooth surfaces. *J. Aerosol Sci.* (2000) 10.1016/S0021-8502(99)00536-4.
11. W. F. Wells, On air-borne infection. Study II. Droplets and droplet nuclei. *Am. J. Hyg.* **20**, 611–618 (1934).

12. X. Xie, Y. Li, A. T. Y. Chwang, P. L. Ho, W. H. Seto, How far droplets can move in indoor environments - revisiting the Wells evaporation-falling curve. *Indoor Air* (2007) 10.1111/j.1600-0668.2007.00469.x.

13. S. Anand, Y. S. Mayya, Size distribution of virus laden droplets from expiratory ejecta of infected subjects. *Sci. Rep.* **10**, 21174 (2020).

14. J. P. Duguid, The size and the duration of air-carriage of respiratory droplets and droplet-nuclei. *J. Hyg. (Lond).* (1946) 10.1017/S0022172400019288.

15. Z. Zuo, *et al.*, Association of airborne virus infectivity and survivability with its carrier particle size. *Aerosol Sci. Technol.* **47**, 373–382 (2013).

16. M. O. Fernandez, *et al.*, Assessing the airborne survival of bacteria in populations of aerosol droplets with a novel technology. *J. R. Soc. Interface* (2019) 10.1098/rsif.2018.0779.

17. V. Stadnytskyi, C. E. Bax, A. Bax, P. Anfinrud, The airborne lifetime of small speech droplets and their potential importance in SARS-CoV-2 transmission. *Proc. Natl. Acad. Sci. U. S. A.* (2020) 10.1073/pnas.2006874117.

18. W. G. Lindsley, *et al.*, Quantity and size distribution of cough-generated aerosol particles produced by influenza patients during and after illness. *J. Occup. Environ. Hyg.* (2012) 10.1080/15459624.2012.684582.

19. L. Morawska, *et al.*, Size distribution and sites of origin of droplets expelled from the human respiratory tract during expiratory activities. *J. Aerosol Sci.* (2009) 10.1016/j.jaerosci.2008.11.002.

20. G. R. Johnson, *et al.*, Modality of human expired aerosol size distributions. *J. Aerosol Sci.* (2011) 10.1016/j.jaerosci.2011.07.009.

21. S. Zhu, S. Kato, J.-H. Yang, Study on transport characteristics of saliva droplets produced by coughing in a calm indoor environment. *Build. Environ.* 41, 1691–1702 (2006).

22. J. Redrow, S. Mao, I. Celik, J. A. Posada, Z. Feng, Modeling the evaporation and dispersion of airborne sputum droplets expelled from a human cough. *Build. Environ.* **46**, 2042–2051 (2011).

23. T. Foat, J. Drodge, J. Nally, S. Parker, A relationship for the diffusion coefficient in eddy diffusion based indoor dispersion modelling. *Build. Environ.* (2020) 10.1016/j.buildenv.2019.106591.

24. V. Vuorinen, *et al.*, Modelling aerosol transport and virus exposure with numerical simulations in relation to SARS-CoV-2 transmission by inhalation indoors. *Saf. Sci.* (2020) 10.1016/j.ssci.2020.104866.

25. J. Yan, *et al.*, Infectious virus in exhaled breath of symptomatic seasonal influenza cases from a college community. *Proc. Natl. Acad. Sci. U. S. A.* (2018) 10.1073/pnas.1716561115.

26. R. Tellier, Y. Li, B. J. Cowling, J. W. Tang, Recognition of aerosol transmission of infectious agents: a commentary. *BMC Infect. Dis.* **19**, 101 (2019).

27. N. van Doremalen, *et al.*, Aerosol and Surface Stability of SARS-CoV-2 as Compared with SARS-CoV-1. *N. Engl. J. Med.* (2020) 10.1056/nejmc2004973.

28. N. A. Fuchs, A. G. Sutugin, Chapter. I. Generation and use of monodisperse aerosols. In Aerosol Science (ed. Davies, C. N.) 1–27, Academic Press, London, (1966).

29. Y. Liu, *et al.*, Viral dynamics in mild and severe cases of COVID-19. *Lancet Infect. Dis.* (2020) 10.1016/S1473-3099(20)30232-2.

30. Mathematica, Version 5.2, Wolfram Research, Inc., Champaign, IL (2005).

31. C. Chen, B. Zhao, Some questions on dispersion of human exhaled droplets in ventilation room: answers from numerical investigation. *Indoor Air* 20, 95–111 (2010).

32. L. Liu, J. Wei, Y. Li, A. Ooi, Evaporation and dispersion of respiratory droplets from coughing. *Indoor Air* (2017) 10.1111/ina.12297.

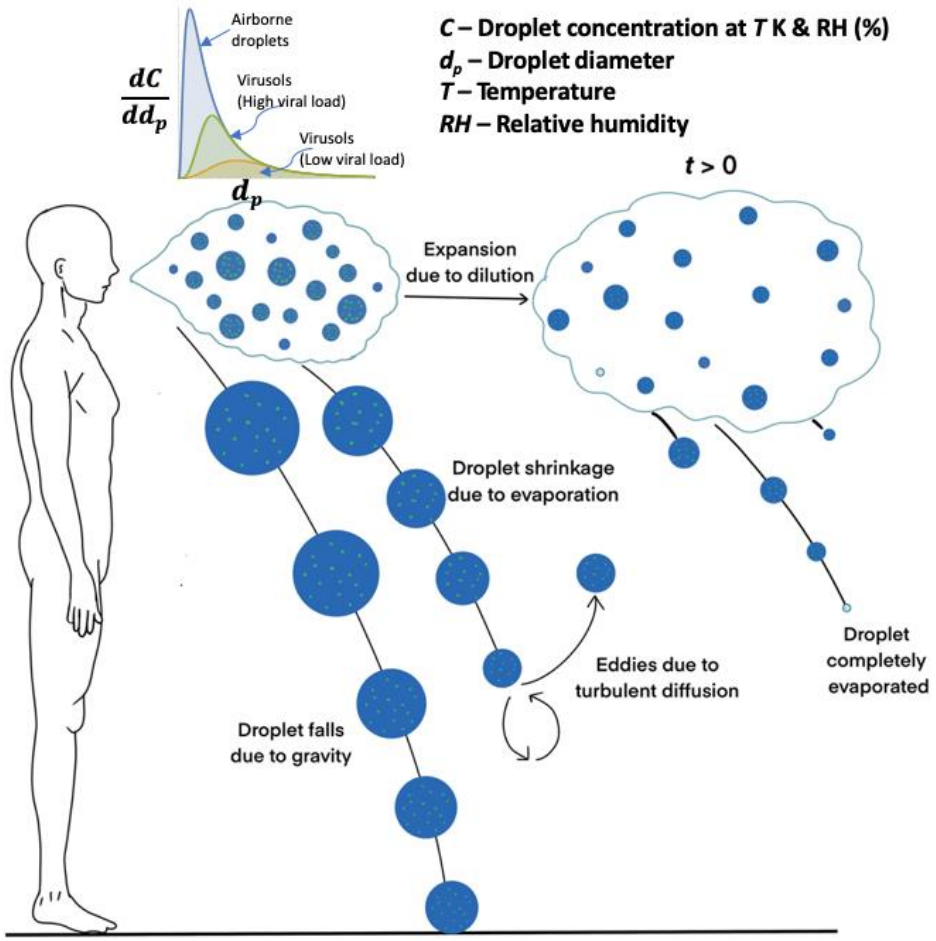

Figure 1. Schematic diagram capturing various physical processes during a typical expiratory event in the indoor environment.

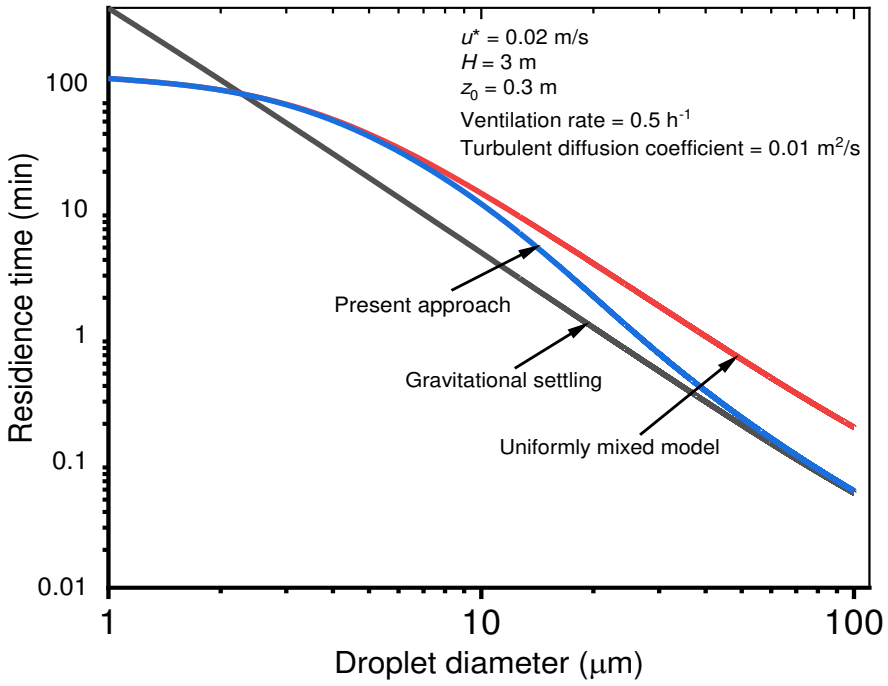

Figure 2. Illustration of the smooth transition of the present model across two limiting models, namely, the uniformly mixed and the falling droplet models, with the variation of droplet size.

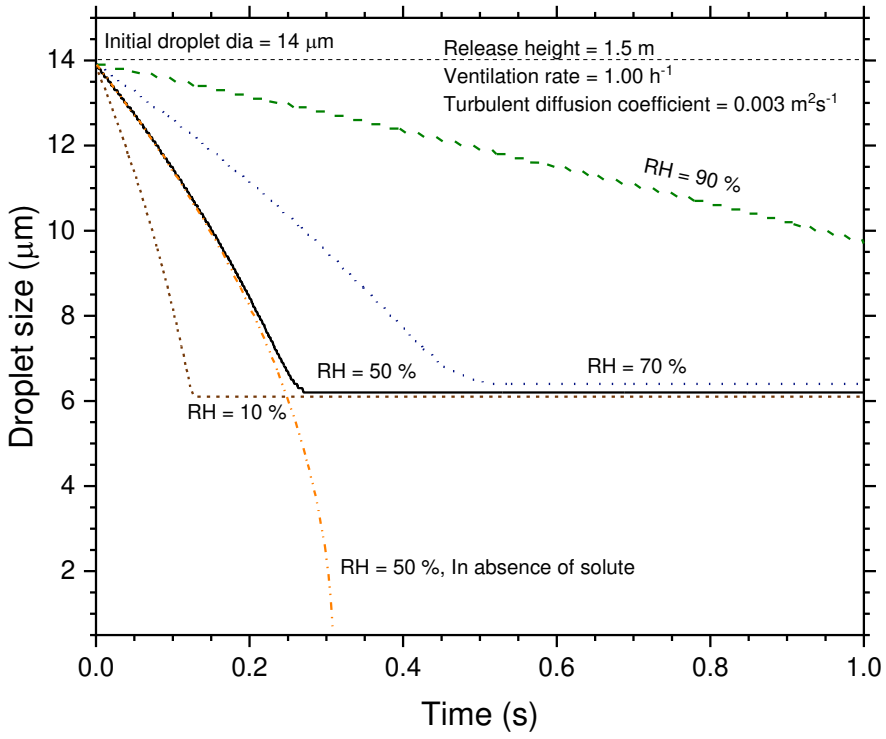

Figure 3a. Temporal evolution of droplet size at different RH.

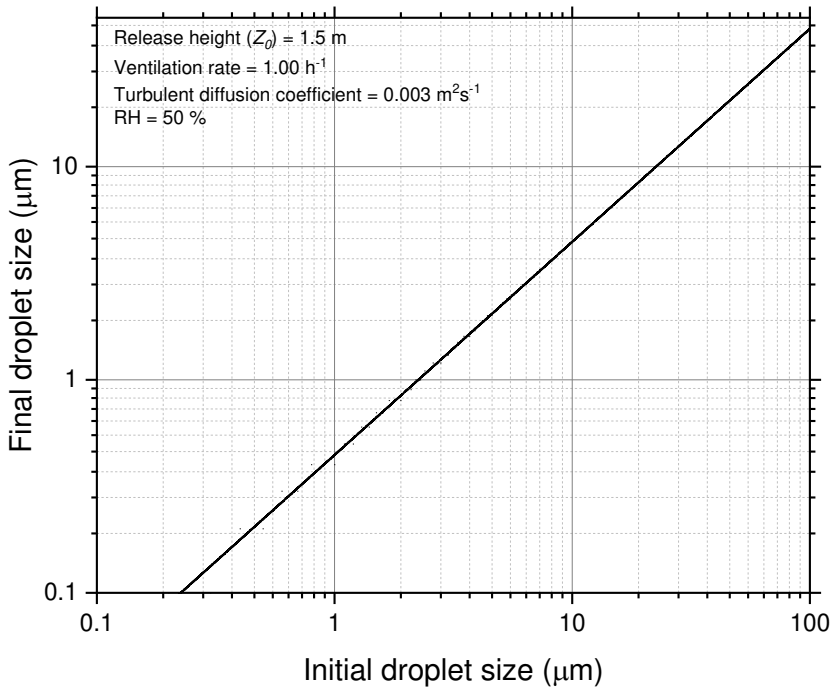

Figure 3b. Residue formation due to evaporation: Initial vs final droplet diameter at 50% RH temperature 25^0C.

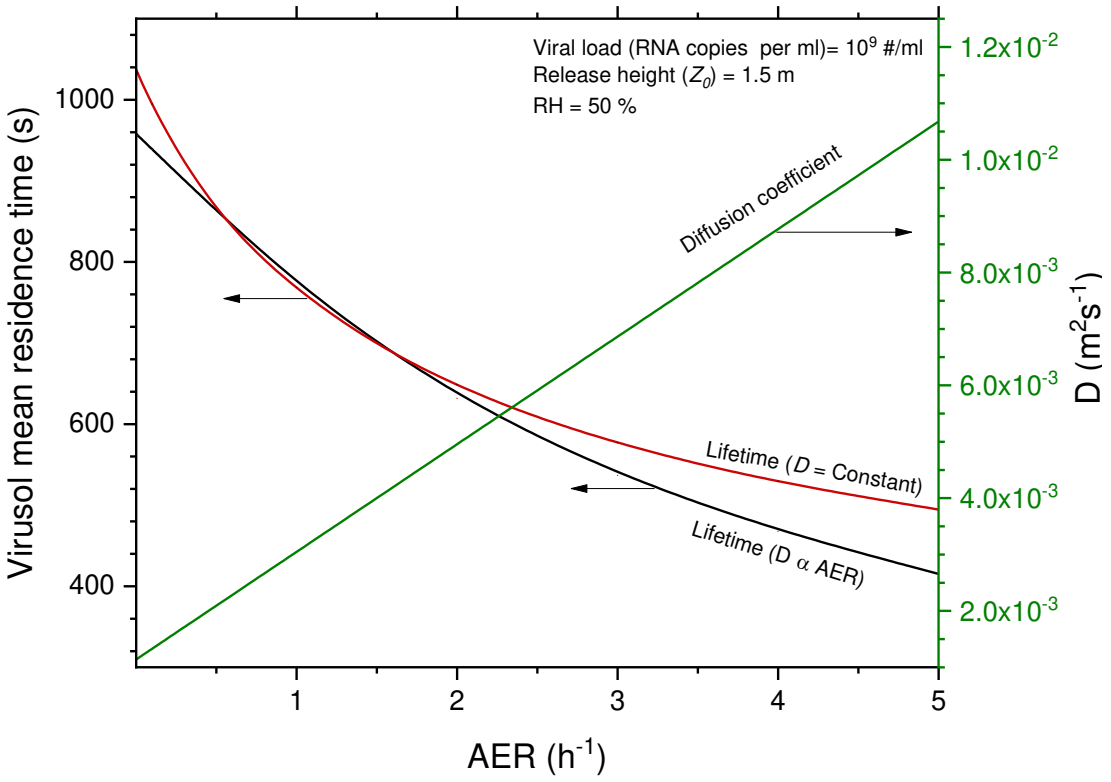

Figure 4. Mean residence time of virusol as a function of diffusion coefficient and AER.

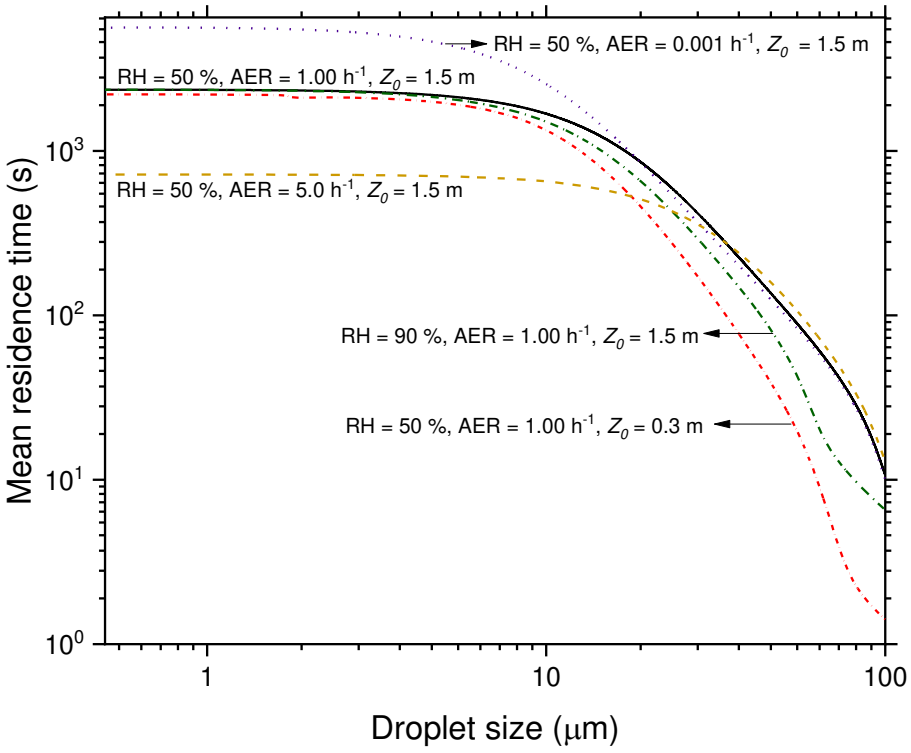

Figure 5. Variation of mean residence time with respect to droplet diameter for different on ventilation rate and release height.

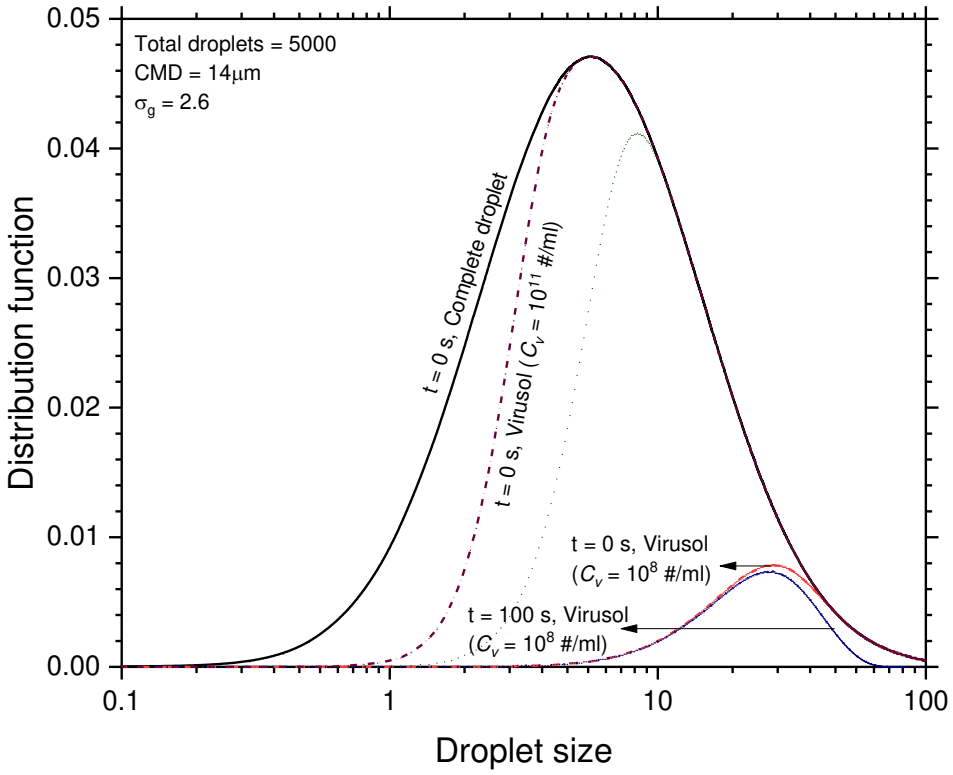

Figure 6. Number-size distribution of cough virusols at t = 0 and t = 100 s for viral load of 10^8 RNA copies/mL, comparison with complete droplet size distribution at t = 0 and virusol size distribution at t = 0 for viral load of 10^{11} RNA copies/mL.

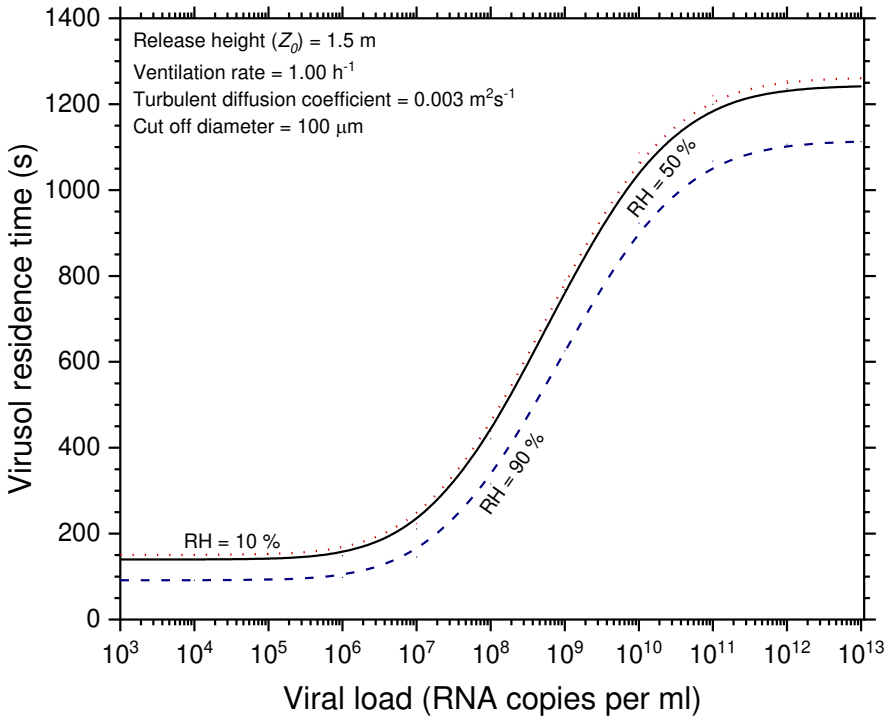

Figure 7. Mean residence time of polydisperse virusol system (original droplet size distribution: CMD – 14 μm and GSD – 2.6) as a function of virus load for different RH.

Supplementary Information (SI)

1. Derivation of analytical solution for the 1-D and 3-D theoretical models, and comparison of their results

2. Table S2: Input Parameters & constants

Figures

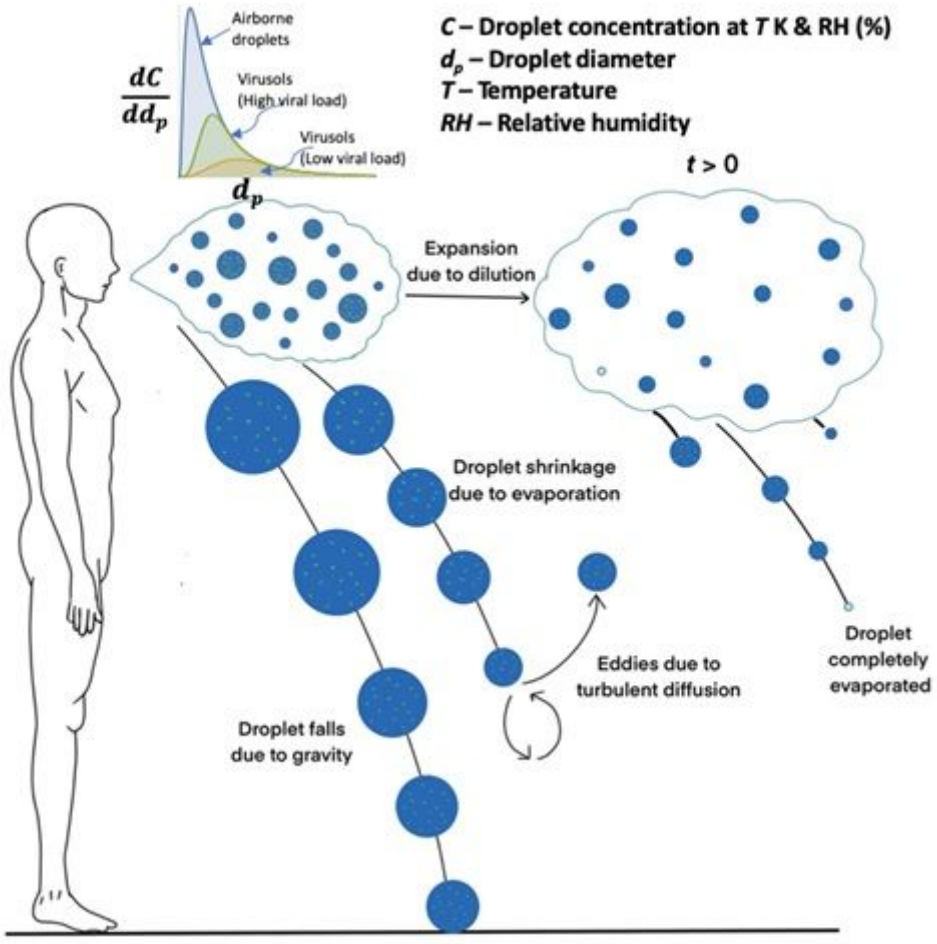

Figure 1

Schematic diagram capturing various physical processes during a typical expiratory event in the indoor environment.

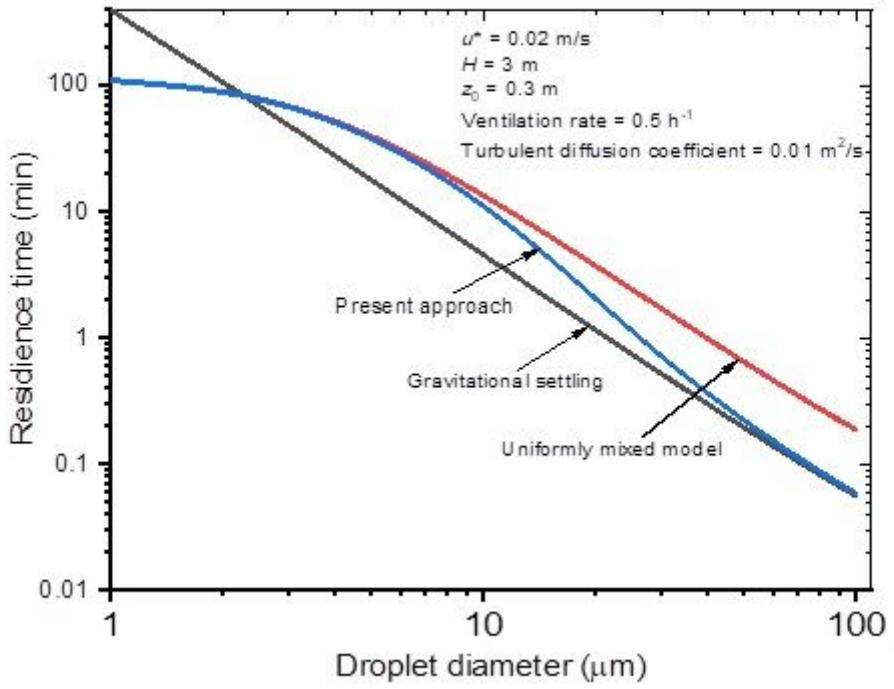

Figure 2

Illustration of the smooth transition of the present model across two limiting models, namely, the uniformly mixed and the falling droplet models, with the variation of droplet size.

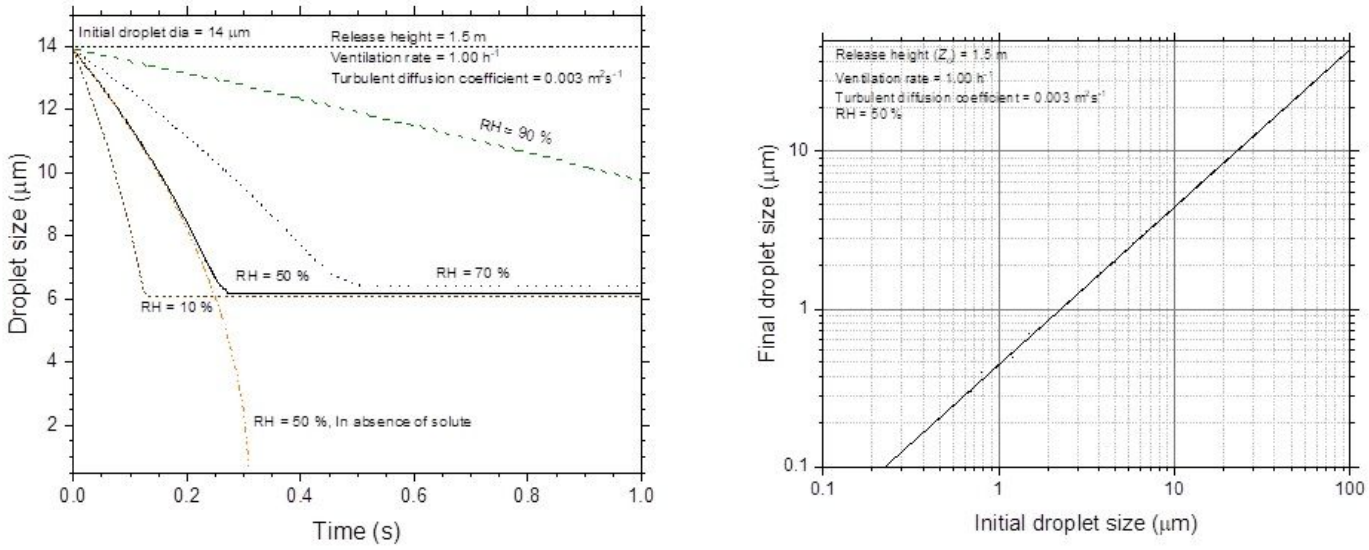

Figure 3

a. Temporal evolution of droplet size at different RH. b. Residue formation due to evaporation: Initial vs final droplet diameter at 50% RH temperature 250C.

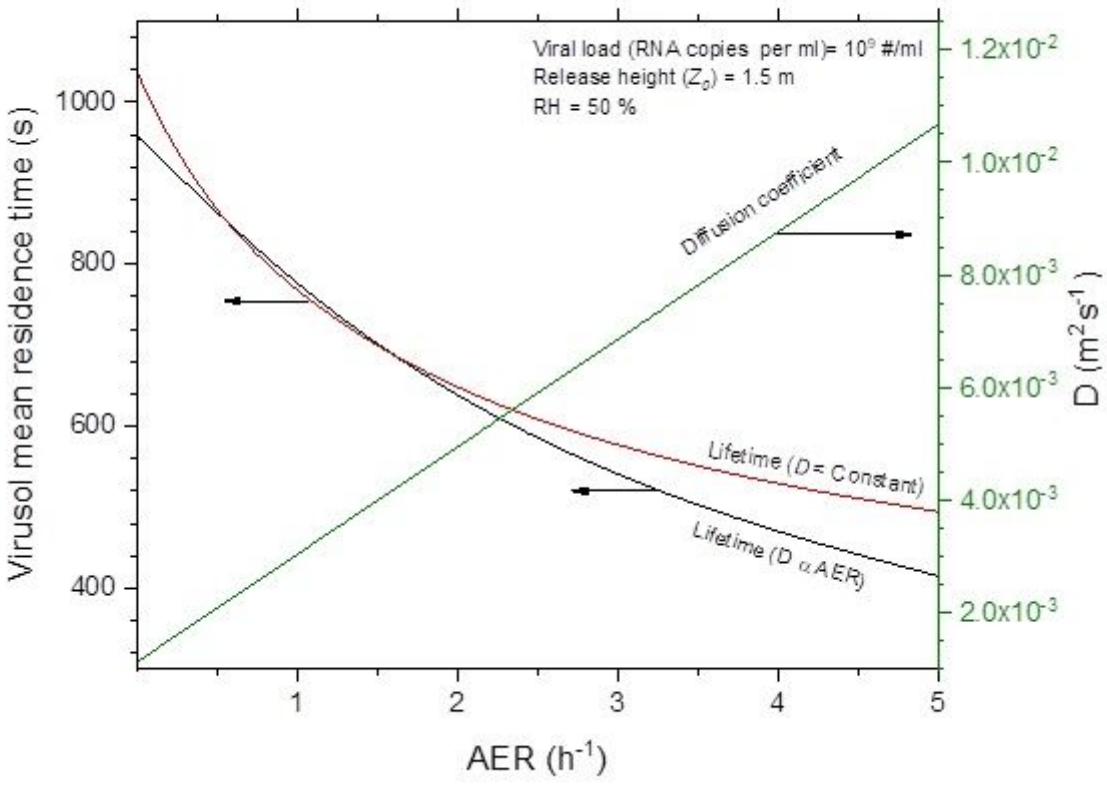

Figure 4

Mean residence time of virusol as a function of diffusion coefficient and AER.

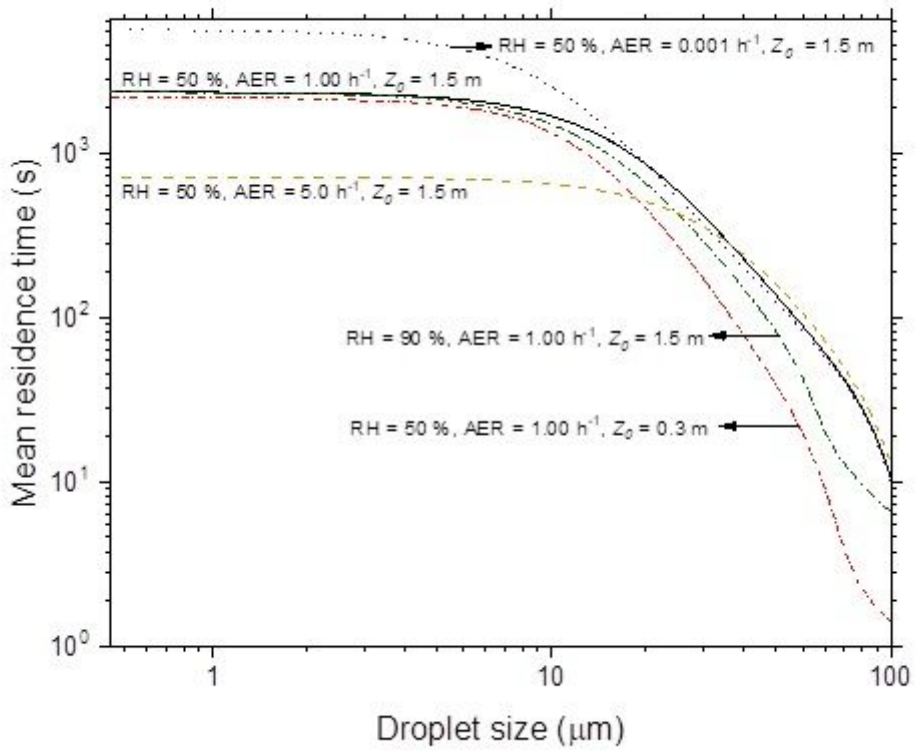

Figure 5

Variation of mean residence time with respect to droplet diameter for different on ventilation rate and release height.

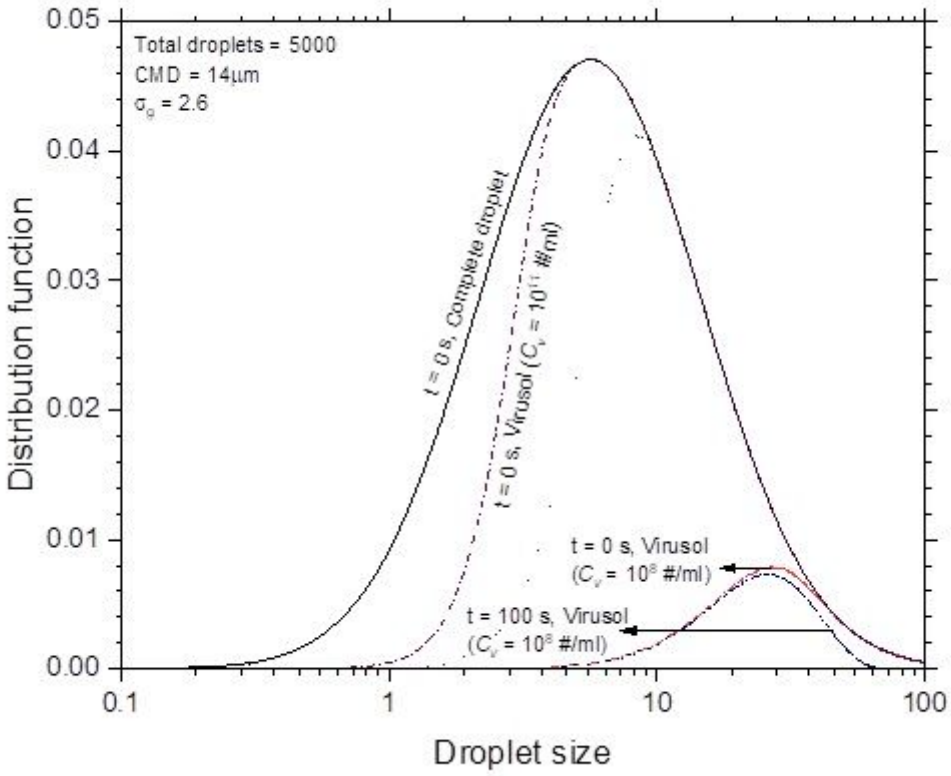

Figure 6

Number-size distribution of cough virusols at t = 0 and t = 100 s for viral load of 108 RNA copies/mL, comparison with complete droplet size distribution at t = 0 and virusol size distribution at t = 0 for viral load of 1011 RNA copies/mL.

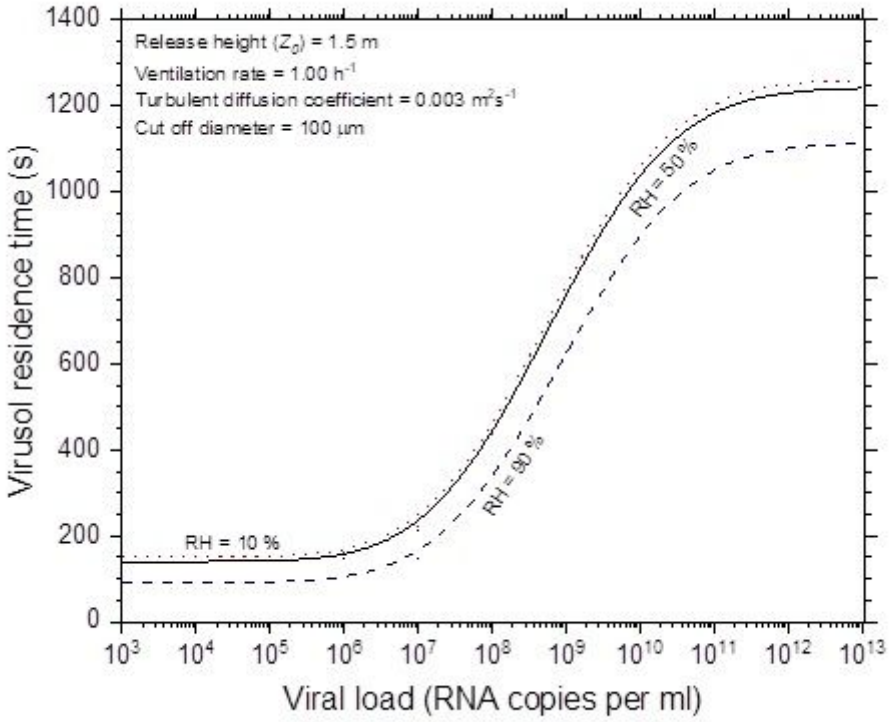

Figure 7

Mean residence time of polydisperse virusol system (original droplet size distribution: CMD – 14 µm and GSD – 2.6) as a function of virus load for different RH.

Supplementary Files

This is a list of supplementary files associated with this preprint. Click to download.

- SupplementaryInformation.docx
- GraphicalAbstract.jpg